JOURNAL OF SOLID STATE CHEMISTRY **129,** 363–366 (1997)
ARTICLE NO. SC977351

# LETTER TO THE EDITOR

# The Nature of Charge Ordering in Rare Earth Manganates and Its Strong Dependence on the Size of the *A*-Site Cations

N. Kumar*,‡ and C. N. R. Rao†,‡,[1]

*Raman Research Institute, Bangalore 560 080, India; †CSIR Center of Excellence in Chemistry, Indian Institute of Science, Bangalore 560 012, India; and ‡Jawaharlal Nehru Center for Advanced Scientific Research, Jakkur, Bangalore 560 064, India

Communicated by J. M. Honig February 12, 1997, accepted February 13, 1997

**Charge ordering in rare earth manganates of the type $Ln_{0.5}A_{0.5}MnO_3$ ($Ln$ = rare earth, $A$ = alkaline earth) is highly sensitive to the average radius of the $A$-site cations, $\langle r_A \rangle$. In the small $\langle r_A \rangle$ regime (e.g., $Y_{0.5}Ca_{0.5}MnO_3$), charge ordering occurs in the paramagnetic state, the transformation to an antiferromagnetic state occurring at still lower temperatures. At moderate $\langle r_A \rangle$ values (e.g., $Nd_{0.5}Sr_{0.5}MnO_3$), a ferromagnetic metallic state transforms to a charge-ordered antiferromagnetic state with cooling. These two distinct types of charge ordering and associated properties are explained in terms of the variation of the exchange couplings $J_{FM}$ and $J_{AFM}$ with $\langle r_A \rangle$ and the invariance of the single-ion Jahn–Teller energy with $\langle r_A \rangle$. A qualitative temperature–$\langle r_A \rangle$ phase diagram, consistent with the experimental observations, has been constructed to describe the properties of the manganates in the different $\langle r_A \rangle$ regimes.**



The concept of charge ordering is not new to transition metal oxides. $Fe_3O_4$ undergoes the well-known Verwey transition at 120 K due to charge ordering and at 860 K due to ferrimagnetic ordering. Charge ordering of the $Mn^{3+}$ and $Mn^{4+}$ ions in the perovskite manganates, $Ln_{1-x}A_xMnO_3$ ($Ln$ = rare earth, $A$ = alkaline earth cation), however, has more dramatic consequences, with the materials exhibiting ferromagnetism and insulator–metal transitions due to $Mn^{3+}$–O–$Mn^{4+}$ double-exchange interaction on one hand and charge ordering and antiferromagnetism on the other (1, 2). The fascinating properties of the manganates arise also in part because $Mn^{3+}$ is a Jahn–Teller ion. Ferromagnetism and charge ordering in the manganates are strongly dependent on the average radius of the $A$-site cations, $\langle r_A \rangle$, which affects the Mn–O–Mn angle and, hence, the $e_g$ bandwidth. The ferromagnetic $T_c$ increases with an increase in $\langle r_A \rangle$, while charge ordering is favored by small $\langle r_A \rangle$. What is truly remarkable is that the magnetotransport properties and the nature of charge ordering in the manganates vary drastically with very small changes in $\langle r_A \rangle$. We shall examine this problem in manganates for a fixed general composition ($Ln_{0.5}A_{0.5}MnO_3$).

When the $\langle r_A \rangle$ is sufficiently large, as in $La_{0.5}Sr_{0.5}MnO_3$ ($\langle r_A \rangle = 1.26$ Å), the manganates become ferromagnetic and undergo an insulator–metal transition around $T_c$. $Nd_{0.5}Sr_{0.5}MnO_3$ with a slightly smaller $\langle r_A \rangle$ (1.236 Å) becomes ferromagnetic and metallic at 250 K ($T_c$) and transforms to a charge-ordered, antiferromagnetic state at 150 K (3). The charge ordering transition temperature, $T_{CO}$, is the same as $T_N$. A significant specific heat anomaly occurs at $T_{CO}$ ($T_N$) and the resistivity increases markedly due to the metal–insulator (FM–CO) transition (Fig. 1). This situation is to be contrasted with that of $Nd_{0.5}Ca_{0.5}MnO_3$ ($\langle r_A \rangle =$ 1.17 Å) which exhibits a $T_{CO}$ of 250 K in the paramagnetic state (4), exhibiting a small heat capacity anomaly; this manganate is an insulator at all temperatures (Fig. 1). $Y_{0.5}Ca_{0.5}MnO_3$ with a $\langle r_A \rangle$ of 1.13 Å becomes charge ordered in the paramagnetic state ($T_{CO}$, 240 K) and becomes antiferromagnetic at 140 K ($T_N$). In Fig. 2 we show a simple diagram where we delineate the different types of behavior of the manganates, depending on $\langle r_A \rangle$. The charge-ordered state of $Nd_{0.5}Sr_{0.5}MnO_3$ is destroyed by application of magnetic fields, rendering the material metallic (3). On the other hand, a magnetic field of 6 T has almost no effect on the charge-ordered insulating state of $Y_{0.5}Ca_{0.5}MnO_3$ (5). Clearly, the charge-ordered states in $Nd_{0.5}Sr_{0.5}MnO_3$ and $Nd_{0.5}(Y_{0.5})Ca_{0.5}MnO_3$ are of different kinds, the difference being attributed to the change in $\langle r_A \rangle$.

The occurrence of two types of CO states can be understood qualitatively in terms of the variation of the exchange couplings, $J_{FM}$, $J_{AFM}$, and of the single-ion Jahn–Teller energy ($E_{JT}$) with $\langle r_A \rangle$. While $J_{FM}$ and $J_{AFM}$ would decrease with a decrease in $\langle r_A \rangle$, albeit with different slopes, $E_{JT}$ would be insensitive to $\langle r_A \rangle$. In the small $\langle r_A \rangle$ regime,

[1] To whom correspondence should be addressed.



0022-4596/97 $25.00

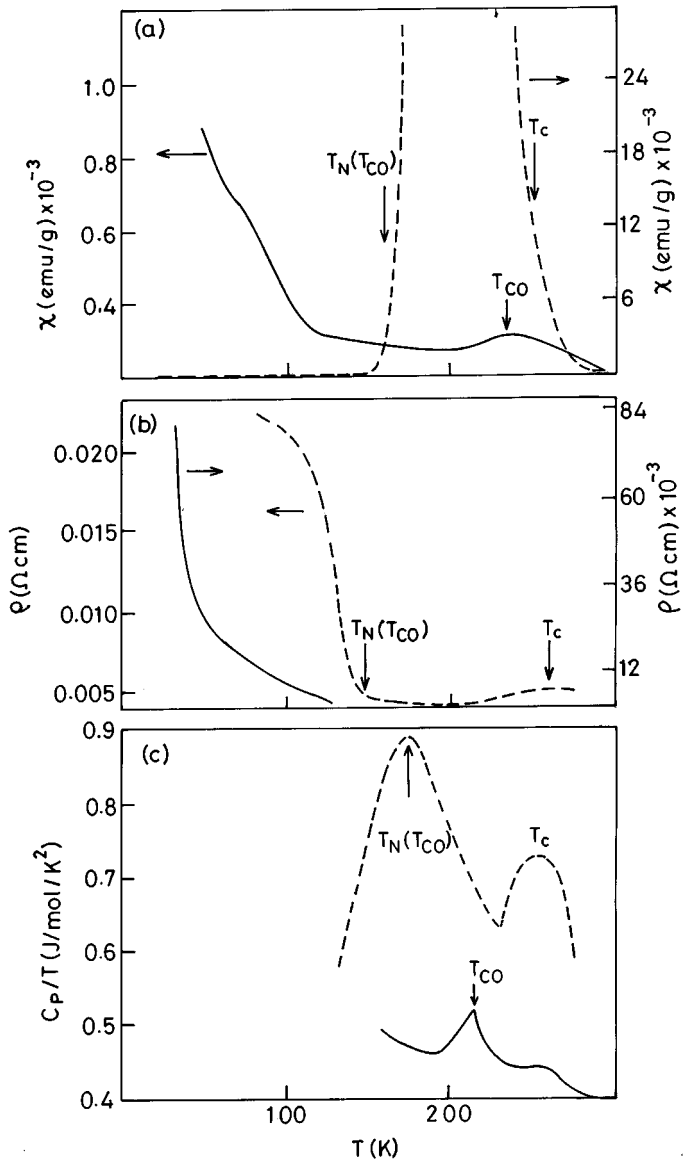


**FIG. 1.** Comparison of the properties of $Nd_{0.5}Sr_{0.5}MnO_3$ ($\langle r_A \rangle$ = 1.236 Å) and $Nd_{0.5}Ca_{0.5}MnO_3$ ($\langle r_A \rangle$ = 1.17 Å). Data represented by broken curves correspond to the former.

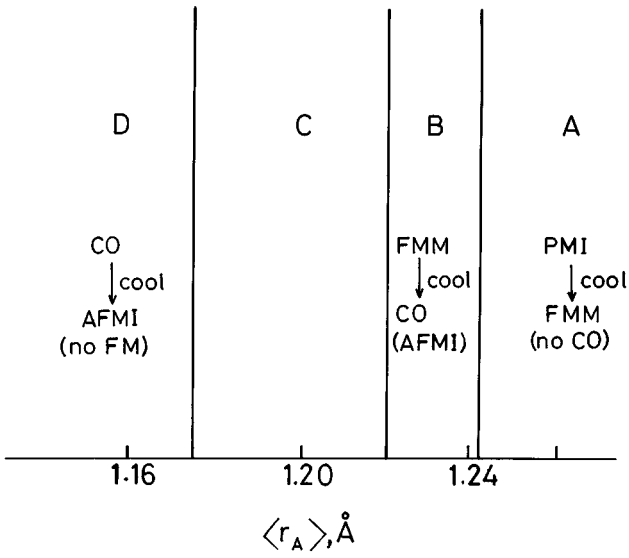


**FIG. 2.** Schematic diagram showing different types of behavior of the manganates, $Ln_{0.5}A_{0.5}MnO_3$, depending on $\langle r_A \rangle$. Region A corresponds to the manganates which show ferromagnetism and insulator–metal transitions at $T_c$ while regions B and D correspond to $Nd_{0.5}Sr_{0.5}MnO_3$ and $Y_{0.5}Ca_{0.5}MnO_3$, respectively. Region C would show complex magnetic and related properties. FMM, ferromagnetic metal; PMI, paramagnetic insulator; AFMI, antiferromagnetic insulator; CO, charge-ordered state.

charge ordering associated with a cooperative Jahn–Teller effect involving long-range elastic strains would dominate, while at moderate values of $\langle r_A \rangle$ (when $J_{AFM} > E_{JT}, J_{FM}$), the $e_g$ electrons which are localized magnetically (due to the spinorial $\cos\theta/2$ blocking) lower the configuration energy by charge ordering. The latter CO state, exemplified by $Nd_{0.5}Sr_{0.5}MnO_3$, would be sensitive to magnetic fields, unlike the small $\langle r_A \rangle$ regime manganates such as $Y_{0.5}Ca_{0.5}MnO_3$. In $Nd_{0.5}Sr_{0.5}MnO_3$, the gain in Zeeman energy resulting from the application of a magnetic field stabilizes the ferromagnetic metallic state over the antiferromagnetic insulating state. The manganates in the small $\langle r_A \rangle$ regime can be considered to involve a pseudo-(Ising)-spin fluid wherein the pseudo-spins (representing the single ion JT effect) do not couple to the magnetic field. That is, the $e_g$ electrons carry, in addition to a magnetic spin, a pseudo-(Ising)-spin, and the two types of CO states derive from the competition between the orderings of the spin and the pseudo-spin fluids. In what follows, we shall elaborate on the $\langle r_A \rangle$ dependence of charge ordering in $Ln_{0.5}A_{0.5}MnO_3$ and describe a plausible temperature–$\langle r_A \rangle$ phase diagram.

A general phase diagram for a fixed composition of the manganates ($Ln_{0.5}A_{0.5}MnO_3$) in the temperature ($T$)–$\langle r_A \rangle$ plane can be constructed from a knowledge of the manner in which $J_{FM}$ and $J_{AFM}$ vary with $\langle r_A \rangle$. We know that the ferromagnetic $T_c$ decreases with $\langle r_A \rangle$ more markedly than the $T_N$ values in the manganates. Thus, the $T_c$ values of $Nd_{0.5}Sr_{0.5}MnO_3$ ($\langle r_A \rangle$ = 1.236 Å) and $La_{0.5}Ca_{0.5}MnO_3$ ($\langle r_A \rangle$ = 1.198 Å) are 250 and 225 K, respectively, while in $Nd_{0.25}La_{0.25}Ca_{0.5}MnO_3$ ($\langle r_A \rangle$ = 1.185 Å) it is 140 K (6). The $T_N$ values of $Nd_{0.5}Sr_{0.5}MnO_3$ and $Y_{0.5}Ca_{0.5}MnO_3$ ($\langle r_A \rangle$ = 1.13 Å) are 150 and 140 K respectively, suggesting that $J_{FM}$ decreases more markedly with $\langle r_A \rangle$ than $J_{AFM}$. Based on these considerations, we have drawn a qualitative phase diagram in Fig. 3. We see that the highest temperature phase is always a paramagnetic insulator (PMI) which is paradistortive (PD). The insulating behavior (or hopping transport) results from the single-ion Jahn–Teller distortion, as well as from the blocking of hopping by strong

Hund coupling to the paramagnetically disordered Mn spins. The high-temperature PD phase is well established in tetragonal rare earth zircons (7). In the manganates, however, we have a pseudo-(Ising)-spin fluid because of the hopping of the carriers.

An examination of the different regions of the phase diagram in Fig. 3 is instructive. In region I, we have the PMI–FMM transition with cooling, as in many of the manganates exhibiting giant magnetoresistance; this region corresponds to region A in Fig. 2. In region II, $J_{AFM} > J_{FM}$, but the extra entropy of the itinerant carriers in the FM state favors the metallic phase. At low temperatures, however, there should occur a first-order FMM–AFMI transition, the latent heat per $Mn^{3+}$ being $\sim k_B T \ln 2$. Region II corresponds to region B of Fig. 2 and is exemplified by $Nd_{0.5}Sr_{0.5}MnO_3$. In region III, $J_{FAM}$ dominates and a first-order PMI–AFMI transition can occur. At low temperatures, there would be charge ordering. Complex magnetic properties can be found in regions III and IV (corresponding to region C in Fig. 2) arising from the coupling with other parameters (e.g., ferroelasticity). CO–FM transitions found in $Nd_{1-x}Sm_xMnO_3$ (8) and $Nd_{0.25}La_{0.25}Ca_{0.5}MnO_3$ (6), as well as canted spin insulating states found in some manganates, can be understood in this manner. There is a possibility of a second-order transition from a PD to a FD phase in region III. Note that charge ordering in region III is induced by the confinement of carriers by the AFM ordering of the Mn spins, which, along with Hund coupling, introduces a spinorial blocking of the $Mn^{3+}$–O–$Mn^{4+}$ carrier transfer. The associated lattice distortion favors charge ordering. Region V is dominated by Jahn–Teller effects wherein the pseudo-(Ising)-spin fluid (PD with carrier hopping) undergoes a first-order transition (due to loss of communal entropy) with cooling to a FD-insulating phase. In the latter, the pseudo-spin direction and position become frozen, giving rise to both orientational and translational ordering. The possibility of a JT glass cannot be ruled out in this region. Region V corresponds to region D in Fig. 2 and is exemplified by $Y_{0.5}Ca_{0.5}MnO_3$. Charge ordering in Region V is distinctly different from that in region II, as is indeed observed experimentally.

Both types of charge ordering discussed above differ from the charge density wave (CDW)-type ordering caused by Fermi-surface nesting. These are more like the infinitely adaptive structures (9, 10) and would occur over a continuous range of doping. Such lattice effects have been found in $La_{0.5}Ca_{0.5}MnO_3$ (11) and $Nd_{0.25}La_{0.25}Ca_{0.5}MnO_3$ (6). If one considers the blocking of the delocalization of $e_g$

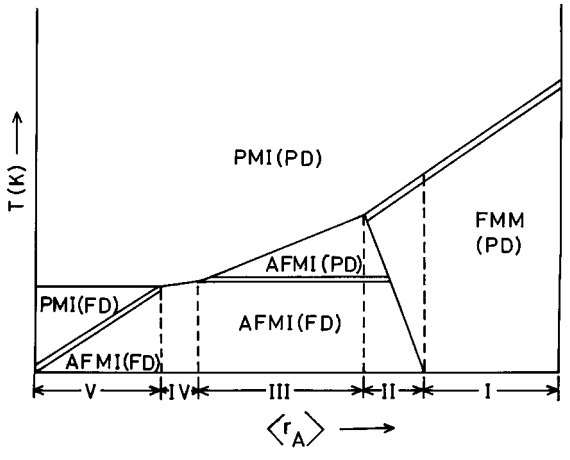


**FIG. 3.** Schematic temperature–$\langle r_A \rangle$ phase diagram for $Ln_{0.5}A_{0.5}MnO_3$ showing different possible behaviors. The double line represents a second-order transition and the single line a first-order transition. PD, paradistortive; FD, ferrodistortive.

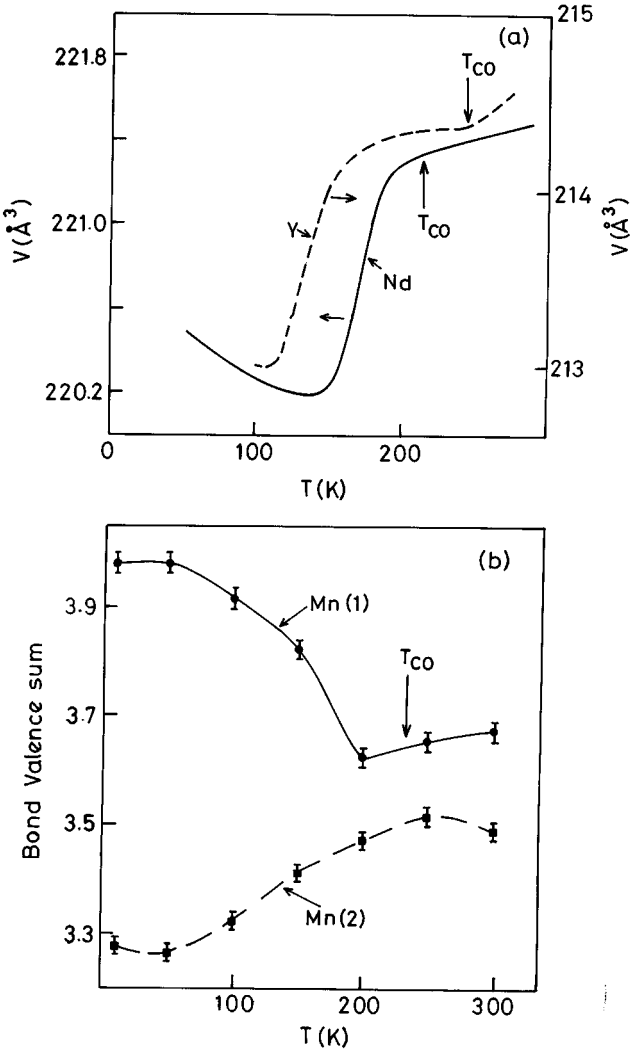


**FIG. 4.** Temperature variation of (a) the unit cell volumes of $Ln_{0.5}Ca_{0.5}MnO_3$ ($Ln$ = Nd and Y) and (b) the bond valence sums in $Nd_{0.5}Ca_{0.5}MnO_3$.

electrons by AFM or JT effects as an enhancement of the effective carrier mass, the CO state may indeed by viewed as Wigner crystallization at low temperatures, even for high carrier concentrations.

We have discussed the phase diagram where $J_{FM}$ decreases faster than $J_{AFM}$ with decreasing $\langle r_A \rangle$. One can construct a phase diagram for the opposite case too, but such a situation may be unlikely. A Ginzburg–Landau description can also be derived having the three competing order parameters (FM, AFM, pseudo-spin FD), with the proviso that the charge-ordered AFMI and FDI phases have no communal entropy, normally associated with the mobile charge carriers.

A comment on charge localization and its relation to charge ordering would be in order. In $Fe_3O_4$, there is little charge localization below the Verwey transition and electrons continue to hop between $Fe^{2+}$ and $Fe^{3+}$ ions down to low temperatures, suggesting a quantum Wigner crystal. In the charge-ordered manganates, localized charges of $Mn^{3+}$ and $Mn^{4+}$ are actually attained at very low temperatures as shown in Fig. 4, for the case of $Nd_{0.5}Ca_{0.5}MnO_3$ (4). Interestingly, such charge-ordered manganates (region V in Fig. 3 and region D in Fig. 2) show gradual but large changes ($\gtrsim 0.5\%$) in the unit cell volume with decreasing temperature, and there is no sharp change at $T_{CO}$ (Fig. 4).

## REFERENCES


1. Y. Tokura, Y. Tomioka, H. Kuwahara, A. Asamitsu, Y. Moritomo, and M. Kasai, *J. Appl. Phys.* **79,** 5288 (1996) and references therein.
2. C. N. R. Rao, A. K. Cheetham, and R. Mahesh, *Chem. Mater.* **8,** 2421 (1996) and references therein.
3. H. Kuwahara, Y. Tomioka, A. Asamitsu, Y. Moritomo, and Y. Tokura, *Science* **270,** 961 (1995).
4. T. Vogt, A. K. Cheetham, R. Mahendiran, A. K. Raychaudhuri, R. Mahesh, and C. N. R. Rao, *Phys. Rev. B* **54,** 15,303 (1996).
5. A. Arulraj, R. Gundakaram, N. Gayathri, A. K. Raychaudhuri, and C. N. R. Rao, to be published.
6. C. N. R. Rao, A. Arulraj, R. Mahesh, R. Gundakaram, N. Y. Vasanthacharya, and N. Rangavittal, to be published.
7. F. Mehran, K. W. H. Stevens, and T. S. Plasket, *Phys. Rev. Lett.* **37,** 1403 (1976).
8. Y. Tokura, H. Kuwahara, Y. Moritomo, Y. Tomioka, and A. Asamitsu, *Phys. Rev. Lett.* **76,** 3184 (1996).
9. C. N. R. Rao and B. Raveau, "Transition Metal Oxides." VCH, New York, 1995.
10. C. Kittel, *Solid State Commun.* **25,** 519 (1978).
11. P. G. Radaelli, D. E. Cox, M. Marezio, S. W. Cheong, P. E. Schiffer, and A. P. Ramirez, *Phys. Rev. Lett.* **75,** 4488 (1995).